Agricultural Water Management 203 (2018) 105–114

Contents lists available at ScienceDirect

Agricultural Water Management

journal homepage: www.elsevier.com/locate/agwat

Water use of Al Ghaf (*Prosopis cineraria*) and Al Sidr (*Ziziphus spina-christi*) forests irrigated with saline groundwater in the hyper-arid deserts of Abu Dhabi

Wafa Al Yamani[a,e], Steve Green[b], Rommel Pangilinan[a], Steve Dixon[c], Shabbir A. Shahid[d], Peter Kemp[e], Brent Clothier[b,*]

[a] *Environment Agency, Abu Dhabi, United Arab Emirates*
[b] *The New Zealand Institute for Plant & Food Research Limited, Palmerston North, New Zealand*
[c] *Maven International, Wellington, New Zealand*
[d] *International Center for Biosaline Agriculture, Dubai, United Arab Emirates*
[e] *Massey University, Palmerston North, New Zealand*

A R T I C L E I N F O

Keywords:
Hyper-arid forests
Saline-water irrigation
Sap flow
Evapotranspiration
Irrigation regulation
Allocation limits

A B S T R A C T

The arid forests of Abu Dhabi provide a variety of valuable provisioning, regulating and cultural ecosystem services. They require irrigating. And groundwater is the source. About 95 % of groundwater consumption is for agriculture and forestry. Over-extraction threatens groundwater resources. The Government of Abu Dhabi recently passed Law 5 to restrict groundwater abstraction. We have determined the minimum allocation required for the irrigation of two tree species. We carried out experiments at Madinat Zayed in the western desert on two arid-forest species: Al Ghaf (*Prosopis cineraria*) and Al Sidr (*Ziziphus spina-christi*), both planted on a 7 m × 7 m grid. We measured the actual evapotranspiration (*ETc*) using heat-pulse equipment in the trees. Saline groundwater with an electrical conductivity of about 8–10 $dS\,m^{-1}$ was used for irrigation. Current practice is to drip irrigate with 60 $L\,d^{-1}$. Both species displayed distinct, and different, summer 'deciduous behaviours' that determine their seasonal pattern of *ETc*. A single crop-factor approach, using *ETc* predicted from *Kc.ETo*, where *Kc* is the crop factor and *ETo* is the reference evaporation, would not provide appropriate irrigation allocations. From our hourly measurements of *ETc*, made over 3 years, we quantified the seasonal pattern in *Kc*. For Al Ghaf, *Kc* ranged from 0.1 during February–July, to 0.15 in November–December; for the Sidr, *Kc* was at a minimum of 0.06 in May, and rose to 0.16 in December. Daily irrigation requirements were provided for Law 5. With a 25% factor-of-safety, and a 25% salt-leaching requirement, irrigation requirements for Al Ghaf ranged from 24.4 $L\,d^{-1}$ in January to 52.8 $L\,d^{-1}$ in July. For Al Sidr the range was from 33.8 $L\,d^{-1}$ in April to 53.5 $L\,d^{-1}$ in September. These are a 40% saving on current practice.

1. Introduction

Groundwater (GW) is the main natural water-resource in Abu Dhabi. It is mostly a non-renewable resource (Murad et al., 2007; Al Mulla 2011). Groundwater has been extensively extracted to meet Abu Dhabi's water needs for various purposes. About 95 % of the total groundwater consumption is used by agriculture and forestry (EAD, 2016b). Over-extraction threatens groundwater sustainability. Abu Dhabi seeks to meet the increased demands for water and avoid further deterioration of groundwater quantity and quality (Murad, 2010; Dawoud, 2011). Environment Agency – Abu Dhabi (EAD) is the government entity mandated to protect and enhance groundwater resources in the Emirate. Their target by 2020 is to reduce the total volume of groundwater extracted annually from 2.198 Mm^3 to 1.82 Mm^3 (EAD, 2016b). The arid forests of Abu Dhabi consume some 11% of the Emirate's groundwater. Arid-forest tree species are also used in landscape amenity-plantings and these use some 14% of Abu Dhabi's groundwater.

The arid forest classification proposed by UNESCO divides arid zones into four categories, based on the ratio of the annual precipitation (P) to the annual potential evapotranspiration (PET). These are Hyper Arid Zones (P/PET ratio < 0.03), Arid Zones ($0.03 < P/PET < 0.2$), Semi-arid zones ($0.2 < P/PET < 0.5$) and Semi-humid zones ($0.5 < P/PET < 0.75$) (De Pauw et al., 2000). Abu Dhabi is hyper-

* Corresponding author.
E-mail address: brent.clothier@plantandfood.co.nz (B. Clothier).

https://doi.org/10.1016/j.agwat.2018.03.006
Received 10 July 2017; Received in revised form 28 February 2018; Accepted 4 March 2018
0378-3774/ © 2018 Elsevier B.V. All rights reserved.

arid, with annual P at around 50 mm, and PET at 2000 mm.

All of the Abu Dhabi arid forests were established more than 35 years ago, and today they provide valuable ecosystem services and benefits to the environment and community. These roles and services provided by Abu Dhabi's arid forests include (FAO, 2010):

- Biodiversity Conservation
- Habitat provision
- Soil stabilization
- Erosion and desertification control
- Climate change mitigation and adaptation
- Providing ecosystem goods such as fodder, wood, herbs and medicines.

Over the last decade, EAD has managed the majority of government forests, along with some private forests in the Emirate of Abu Dhabi. Up until recently, the total planted area is 102,852 ha and comprises more than 19 million trees (EAD, 2016a).

1.1. Groundwater protection and regulation

Unsustainable use of groundwater to irrigate these forests is one of the significant environmental challenges facing Abu Dhabi. It requires urgent intervention, and therefore EAD has made significant decisions. The Agency selected and cancelled some 105 forests in 2016. This is around one third of the number of forest sites and all operational activities, including irrigation, have been stopped in these forests.

Another key strategy for addressing Abu Dhabi's groundwater sustainability includes regulating for the responsible use of the remaining groundwater. In 2017, during the International Water Summit (IWS), EAD announced the new Law No. 5, the Groundwater Organisation Law for Abu Dhabi Emirate, passed by HH Sheikh Khalifa bin Zayed Al Nahyan, the President of the United Arab Emirates. This law states that the Abu Dhabi Government owns the groundwater resources in the Emirate of Abu Dhabi. Also, under this law, groundwater abstraction and usage will be under EAD's control. Abu Dhabi is the first government in the Gulf region to state that it owns groundwater. The main objective of this new law is to ensure proper management of groundwater resources in the Emirate. The goal is to conserve groundwater and to allow the resources to replenish (EAD, 2017).

1.2. Research objectives

In order to achieve a reduction in the use of groundwater to irrigate the arid forests, it is necessary to determine first how much water the trees are actually using, and then determine how this might be reduced. For our research to answer this question we considered it best be undertaken by using direct sap-flow measurements of transpiration in these forests and then using this knowledge to develop irrigation management tools. The main objective of this research is to quantify the water consumption of two arid forest species, Al Ghaf and Al Sidr trees, irrigated with saline groundwater (GW) at salinities typical of the region, namely ≈ 10 dS/m, or 6400 ppm.

Our results will enable the development of strategies for improving the use of saline water in agriculture and can address institutional and regulatory aspects of agricultural water management. We show how our results will be used by EAD in the regulations that have been promulgated through Law 5 in Abu Dhabi.

2. Materials & methods

The major species in the arid forests of the Abu Dhabi desert are Al Ghaf, Al Sidr, Al Arak and Al Samar. These species were chosen in our broader project to be our experimental trees because they are the most widely distributed native plant species in Abu Dhabi forests, covering around 78% of forest plants in the emirate (EAD, 2016a). However, in this paper we will only cover the Ghaf and Sidr trees that have been irrigated with saline groundwater (GW). Further details for each of these tree species are provided below.

2.1. Research site and soil

During December 2014, experiments were set up on two plots of mature Al Ghaf and Al Sidr tree in the Khub al Dahs Forest (23.51° N, 53.75° E) near Madinat Zayed in the Al Dhafra region in the western desert of Abu Dhabi.

The soil type at the experimental site is classified as a Typic Torripsamment, mixed, hyperthermic (Soil AD158) (EAD, 2009). This type of soil is a deep, sandy soil with mixed mineralogy. It is widely distributed across Abu Dhabi with more than 50% of the Emirate having this soil type, and the majority of the arid forests in the Emirate are on this soil type.

A mini-disk infiltrometer (Decagon Devices Inc., Pullman, Washington, USA) was used to measure the soil's near-saturated hydraulic conductivity, K (mm h^{-1}). The 3-D flow of water from the fritted disk of the mini-disk of radius r_o quickly approaches a steady state Q_∞ ($m^3 s^{-1}$). Wooding's equation (Wooding, 1968) describes this steady flow in relation to the disk's radius and the soil's hydraulic conductivity function – if it is of the form

$$K(h) \quad = \quad K_s \exp(\alpha\, h), \tag{1}$$

where h is the soil-water pressure head (mm), K_s is the saturated hydraulic conductivity when $h = 0$, and α is the slope of the exponential $K(h)$ relationship.

Wooding's equation is

$$Q_\infty \quad = \quad K_s\left(\pi\, r_o^2 + \frac{4\, r_o}{\alpha}\right). \tag{2}$$

Measurements of Q_∞ from a minidisk of radius r_o can be used to resolve the soil's hydraulic character. However, the equation contains two unknowns, K_s and α so multiple observations are required (Clothier, 2000). Ankeny et al. (1991) proposed a simultaneous solution of Wooding's equation based on a single permeameter and observations of steady infiltration at the two different heads h_1 and h_2. The infiltration commenced with h_2 first being -60 mm, and then with h_1 being -5 mm. Five replicate measurements of these were made. The structureless, wind-blown sand is spatially quite uniform. The sand was found to be very permeable. The slope α was found to be 0.02 mm^{-1}, and by extrapolation from h_1 to $h = 0$ (Eq. (1)) the saturated hydraulic conductivity K_s was found to be 9 m h^{-1}.

2.2. Drip irrigation

Automatic irrigation systems were installed at both experimental sites to control and manage the irrigation. Two tanks of 22,730 L, one at the Ghaf site and the other at the Sidr site, are filled continuously with GW with salinity of 8–10 dS m^{-1}. The water is then transferred into smaller tanks of 2273 Litres to help in the mixing of the water inside the tanks and reduce salinity variations. Each system was run for 7 h daily, starting early in the morning. Flow meters record the actual amounts of irrigated water. Water is applied to trees using pressure-compensated drippers with two 4 L h^{-1} drippers per tree. Thus each tree would receive just under 60 L d^{-1}, every day of the year.

Because of the permeable nature of this coarse sand, we sought to understand what size the wetted volume of soil would be when irrigated by dripper at 4 L h^{-1} for 7 h. To do this we used Philip's (1984) analytical solution for steady-state travel times away from a surface point source discharging at rate Q (L h^{-1}). This is reasonable, as steady-state conditions develop rapidly during 3-D infiltration, especially close to the emitter (Clothier, 1984). Philip's (1984) solution also assumed an exponential hydraulic conductivity function with slope α (Eq. (1)). The solution depends only on Q, α, and the soil's average water content θ

($m^3\,m^{-3}$).

(Philip, 1984) provided a simple solution, especially the radius of wetting, R, at the surface (depth $Z = 0$), where the expansion of the wet-front with time, T^*, will be:

$$T^*(R, O) = 2 \exp(R)(1 - R + R^2/2) - 2, \quad (3)$$

and for penetration of the wet-front directly under the dripper ($R = 0$):

$$T^*(O, Z) = Z^2/2 - Z + \ln(1 + Z). \quad (4)$$

Here the non-dimensional lengths are $Z = \alpha z$, where z is the depth (m) below the dripper, and $R = \alpha r$ where r (m) is the radial distance from the dripper

The non-dimensional travel time T^* from the origin is

$$T^* = \alpha^3 Qt/(16\pi\theta). \quad (5)$$

The wet-front penetration predictions using Eqs. (3) and (4) are shown in Fig. 1 for $Q = 4\,L\,h^{-1}$, and an average water content in the transmission zone of $0.2\,m^3\,m^{-3}$, and $\alpha = 0.02\,mm^{-1}$. It can be seen that during the 7 h irrigation the wet-front at the surface could be expected to reach about 200 mm away from the dripper. This is what we observed in the field. Underneath the dripper, the wet-front would be expected to extend beyond 0.6 m. So the drippers would wet the soil to some considerable depth, enabling the trees to take up water from deeper down to meet the atmospheric demand for water.

2.3. Soil water and salinity monitoring

Two Campbell CS655 soil-water content reflectometers were installed in the drip zone of both the Ghaf and Sidr plots. One probe was inserted in the drip zone of a GW-irrigated tree and the other in that of a tree irrigated with treated sewage effluent (TSE). The CS655 measures the soil-water content,θ, and bulk electrical conductivity (EC_b, $dS\,m^{-1}$). In a separate laboratory test, we calibrated the CS655 probe to infer the soil-solution EC from both θ and EC_b. The calibration for EC was found to be linear with EC_b and parabolic with θ (Al-Muaini, *pers. comm.*, 2016).

In Fig. 2 we show the daily pattern of θ and EC during the irrigation period (0630–1330) for the GW irrigated Al Ghaf that was instrumented with the CS655 probe. The rapid rise and fall of θ reflects the highly permeable nature of this sand, and rootzone uptake of water to meet the atmosphere's demand on the tree for water. The calibration equation for EC provides erroneous values when the soil is at saturation. After the free-water drains away from the drip zone, the EC can be seen to rise to just over $8\,dS\,m^{-1}$, being about the salinity of the applied water. Here, and throughout the year, at this irrigation rate of about 60 L per tree per day, there is no change in the solution EC value, showing that there is effective flushing of excess salts from the rootzone.

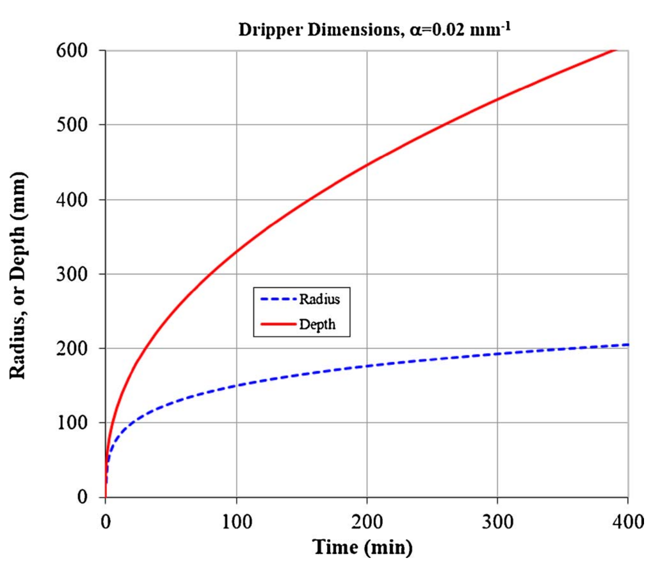

Fig. 1. Predictions using Philip's (1984) theory for the development of the wet-front across the soil surface (Eq. (3)) and below a dripper (Eq. (4)) discharging at $4\,L\,h^{-1}$ onto the surface of sand in the Khub al Dahs forest near Madinat Zayed.

2.4. The tree species

There are 12 trees in each of the 2 plots for Al Ghaf and Al Sidr, and within each plot six trees have been irrigated with GW, and six with treated sewage effluent (TSE). The GW has a salinity of around $10\,dS\,m^{-1}$, whereas the TSE has a salinity of less than $1\,dS\,m^{-1}$. Here we report only on the GW results. Our focus here is to develop water-management protocols for saline groundwaters.

The Ghaf, or Al Ghaf, is the local Arabic name for *Prosopis cineraria*. Al Ghaf tree has a straight unbranched trunk for the first few metres. Then the branching starts. It is an indigenous species of the Arabian Desert. Al Ghaf is a drought-tolerant, evergreen, leguminous tree which can tolerate the harsh climate of the desert environment. However, the Ghaf trees in managed forests are all dependent upon irrigation. Al Ghaf trees can survive even when irrigated with highly saline groundwater. Nevertheless, the degree of salinity does affect their natural growth and health. Despite being evergreen, Al Ghaf undergoes cycles of leaf fall, fruiting and leaf renewal (Khan, 1999).

The Sidr, or Al Sidr, is the local Arabic name for *Ziziphus spina-christi*. The trunk may be undivided or divided near the base. The Sidr tree is frequently multi-branched. Sidr is tolerant to harsh conditions such as salt, drought, desert heat, and even heavy grazing by gazelles and camels (Khan, 1999; EAD, 2006).

2.5. Sapflow monitoring of transpiration

We installed heat-pulse devices in four trees per treatment to provide continuous monitoring of the trees' transpiration (T) using the compensation heat pulse velocity (CHPV) method (Green et al., 2003). We used a standard spacing of the temperature probes of 5 mm upstream and 10 mm downstream from the heater probe. For the larger single-trunk Ghaf trees the temperature sensors in the probes were located at 10, 25, 40 and 55 mm below the cambium. Two sets of devices were installed in each of the four trees. For the thinner and multi-stemmed Sidr trees only two sensors per probe were used and these were located at 5 and 12 mm below the cambium. Four stems were instrumented in each of the four monitored Al Sidr trees.

A Campbell data logger (CR1000, Campbell Scientific, Logan, USA) was used to measure the time taken to achieve temperature equality between sensors located above and below the heater (t_Z, s) following the application of a 2.5 s heat pulse. Data were collected at 30 min intervals. Sap flow ($L\,h^{-1}$) was calculated from measurements of t_Z using the approach outlined by Green et al. (2003), Green et al. (2009). These calculations included a correction for the effect of wounding. A wound diameter of 2.8 mm was used for the 2.0 mm diameter drill holes. Sap velocity was then deduced from the wound-corrected heat-pulse velocity and measured volumetric fractions of wood and water within the sapwood. The fractions of wood (Fm) and water (Fl) in the sapwood were determined gravimetrically from core samples ($Fm = 0.35$ and $Fl = 0.60$). Transpiration (T, $L\,d^{-1}$) was determined by multiplying sap velocity by the conducting wood area using the simple annulus approach suggested by Hatton et al. (1990).

This equipment was installed in the Al Ghaf trees during December 2014, and during February 2015 in the Sidr trees. The experiments have continued through into 2018.

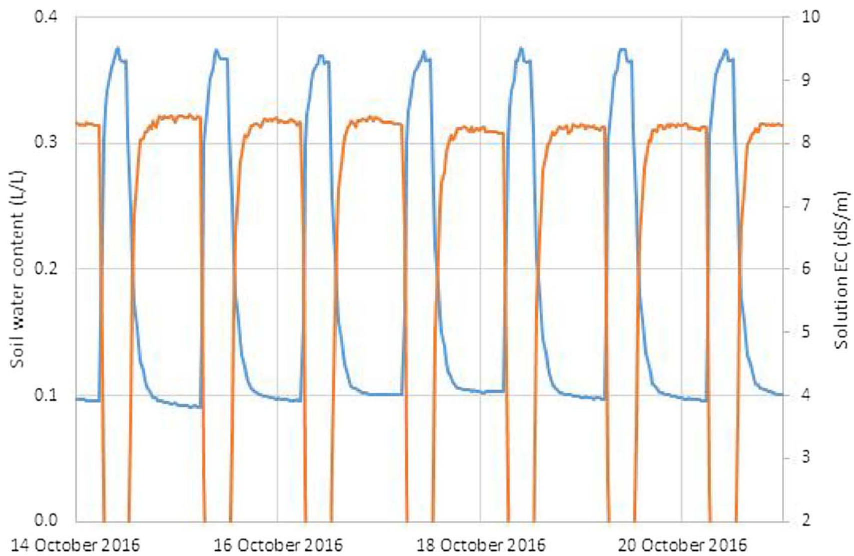

Fig. 2. The diurnal pattern of soil water content, θ, (left axis), and solution EC inferred from the bulk EC_b and θ measured by a Campbell CS655 soil-water reflectometer in the drip zone of a Ghaf tree irrigated with saline groundwater (GW).

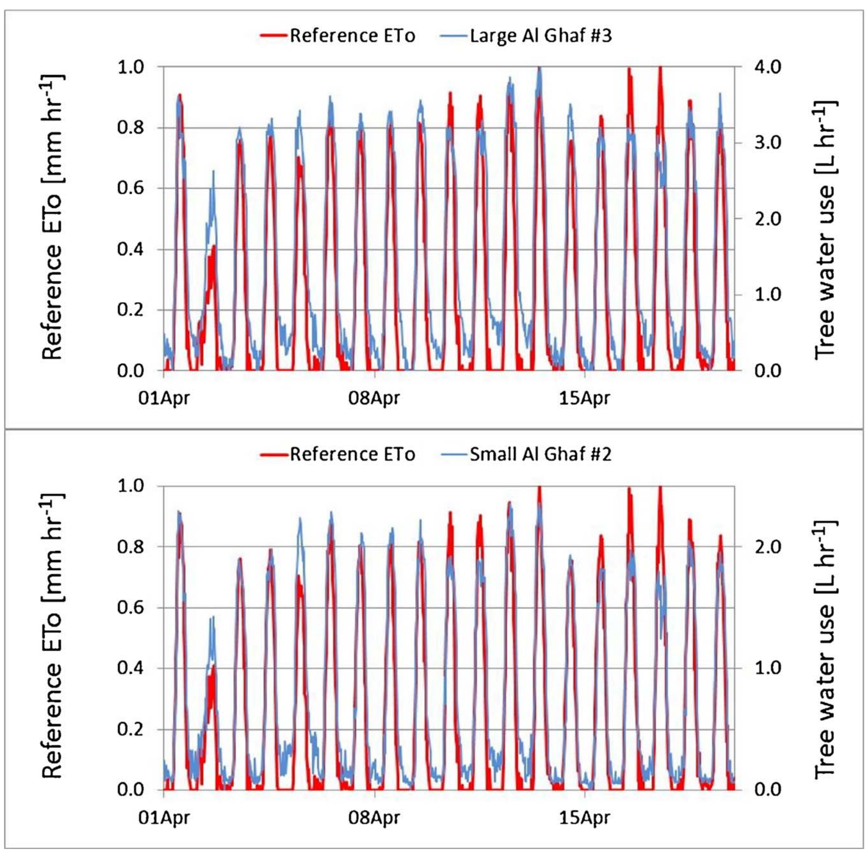

Fig. 3. Top: The measured pattern of the half-hourly tree water use, T (L h^{-1}, right axis), of a large Al Ghaf tree (#3) during the spring of 2015 in relation to the reference ETo (mm h^{-1}, left axis). Bottom: As above, but for a small Al Ghaf (#2) tree. Note the different scale of the right-hand axes between the top and bottom graphs.

2.6. Weather monitoring

The weather station at Khub Al Dahs forest records sub-hourly climate data comprising global shortwave radiation (LiCor 1200), air temperature and relative humidity (Vaisala HMP 45C), wind speed at 3 m (RM Young), and rainfall (TE525 MM-L, Texas Electronics).

These weather data are used to estimate hourly and daily values of the reference evaporation (ETo, mm h^{-1}, or mm d^{-1}) using the standard approach of FAO-56 (Allen, 1998). The transpiration of the trees (ETc, mm h^{-1}, or mm d^{-1}) is then related to ET_O through the dimensionless crop-factor, K_C:

$$ET_c = K_c.\ ET_o. \tag{6}$$

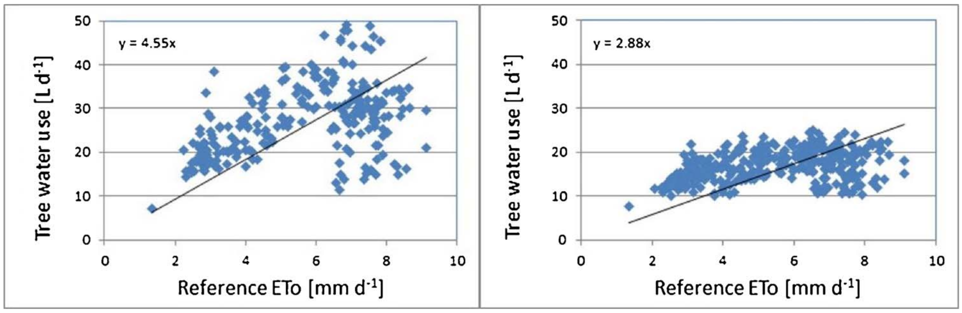

Fig. 4. Left. The regression of the measured daily water-use by Tree 3, *T* in L d^{-1}, against the daily reference *ETo*, in mm d^{-1}. The data set covers 12/12/2014 until 24/11/2015. The slope of the regression is 4.55. Right. As above, but for the smaller Tree 2. The regression slope is 2.88.

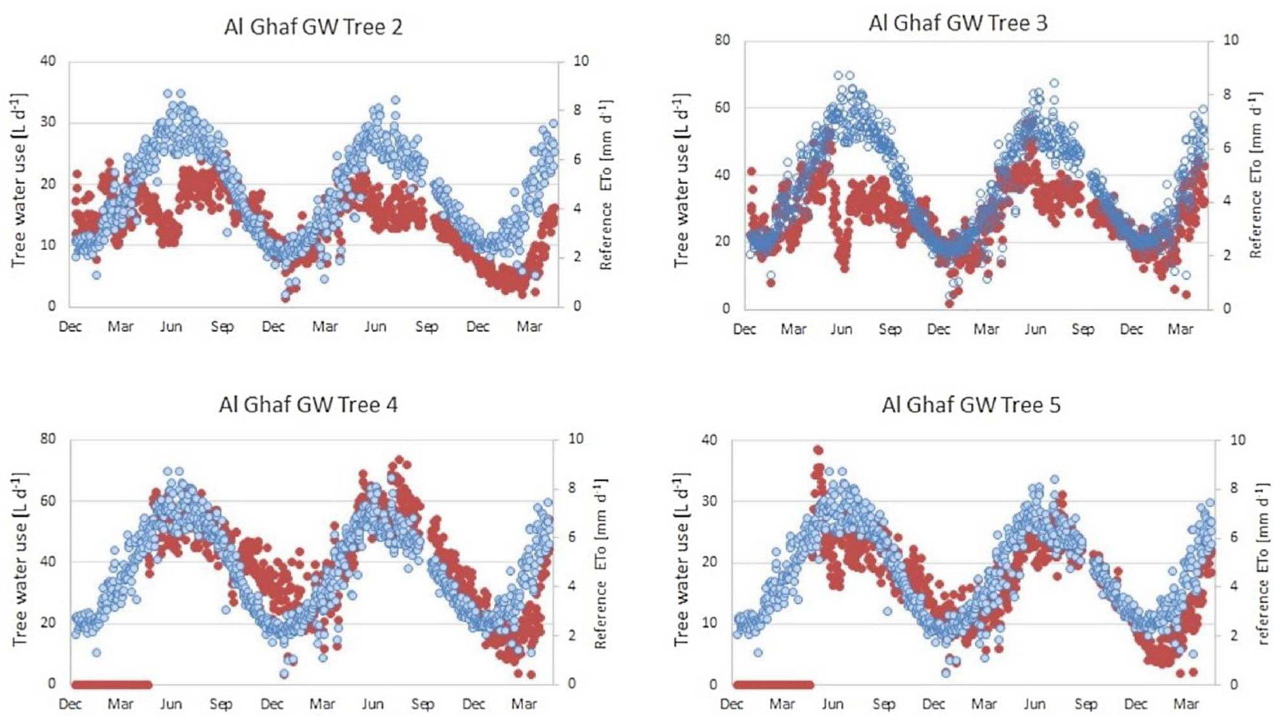

Fig. 5. The seasonal pattern of measured daily water-use *T* (red dots, left axis) for all 4 GW irrigated Al Ghaf trees in relation to *ETo* (blue circles, right axis). The periods cover from late 2015 through until early 2017. Top left: Tree 2; Top right: Tree 3; Bottom left: Tree 4; Bottom right: Tree 5. Note the different scales on left-hand axes for transpiration *T*, in L d^{-1}, due to the different sizes of the four trees. (For interpretation of the references to colour in this figure legend, the reader is referred to the web version of this article.)

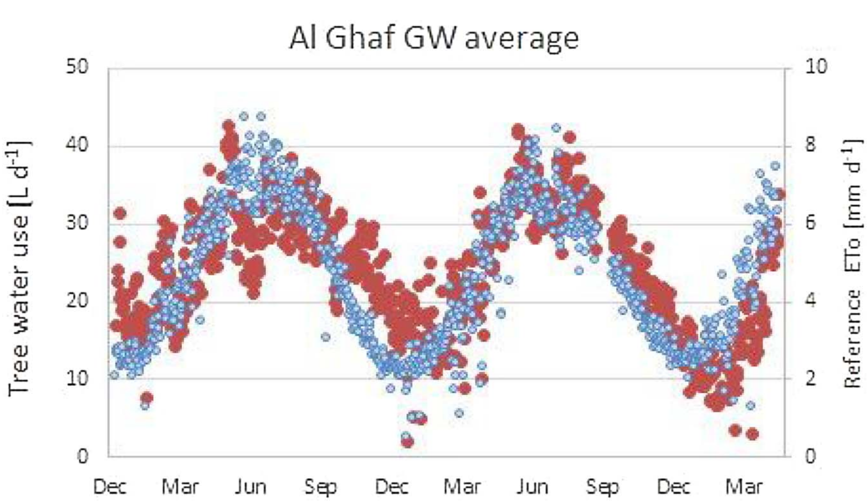

Fig. 6. The seasonal pattern of average of the measured daily water-use *T* (red dots, left axis) for all four GW irrigated Al Ghaf trees in relation to *ETo* (blue circles, right axis). (For interpretation of the references to colour in this figure legend, the reader is referred to the web version of this article.)

Fig. 7. Photographs of two Al Ghaf trees taken on the same day, the 26th of April 2017. The tree on the left (Tree 3) had lost many leaves, showed little emergence of new leaves, and was beginning to flower heavily. The tree on the right (Tree 4) was showing no signs of flowering, but was undergoing a surge in new-leaf growth.

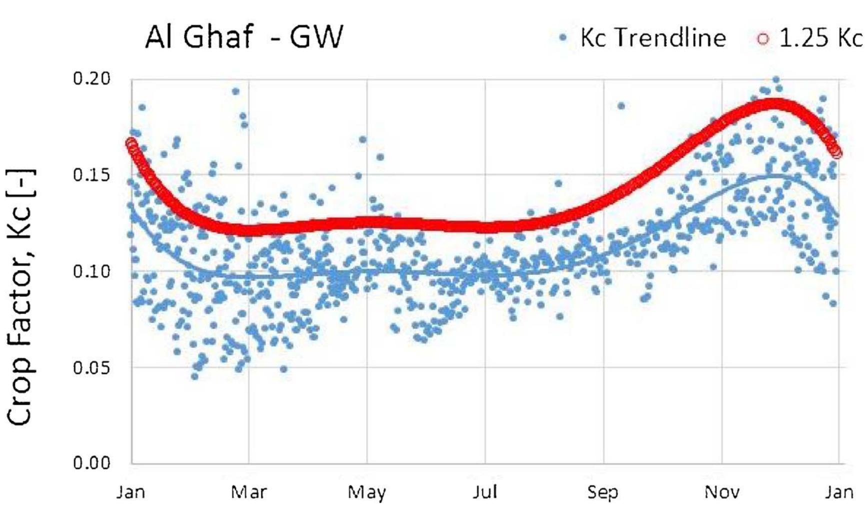

Fig. 8. The average daily crop-factor, *K*c, for the four instrumented Ghaf trees over the year, computed from nearly 2.5 years of individual tree water-use *ET*c. The blue line is the fitted trendline using a 5th order polynomial. The red line is the fitted line with a 25% add-on as a 'factor-of-safety'. (For interpretation of the references to colour in this figure legend, the reader is referred to the web version of this article.)

3. Results and discussion

3.1. Al Ghaf transpiration

Sap flow data for the four GW irrigated Ghaf trees began on 12 December 2014, and continued through until 2017. The four trees are of different sizes, and so we would expect the crop factor, *K*c, to vary between trees. In Fig. 3 (top) we show the hourly transpiration of Tree 3 (in L h^{-1}), one of the largest, in relation to the reference *ET*o (mm h^{-1}), over a period of nearly 3 weeks in the spring of 2014. The vertical axes have been scaled so the traces overlap each other. That the traces do overlap indicates that a single crop factor (Eq. (6)) is appropriate for describing this data set. We have repeated this 'scaling' procedure for the smallest GW-irrigated Ghaf tree (#2), and this is shown in Fig. 3 (bottom). Note the different scales of the right hand axes, which reflects the smaller crop factor for the smaller tree.

The daily value of the crop factor can be quantified by regressing tree water use, *T* in L d^{-1}, against the reference *ET*o in mm d^{-1}. Using a year's data set for both trees from 12 December 2014 until 24 November 2015, we found the slope of the regressions to be 4.55 for the large tree (Tree #3) and 2.88 for the smaller Tree #2 (Fig. 4). Since the trees are planted on a 7 m by 7 m grid, these slopes turn into crop factors of 0.09 (= 4.55/(7 × 7)) for Tree 3, and 0.059 (= 2.88/(7 × 7)) for Tree 2. However, it is clear from the scatter of both plots, that a single annual crop factor, *K*c, would not enable a good prediction of the seasonal pattern of daily tree water use, *ET*c. Indeed, the correlation

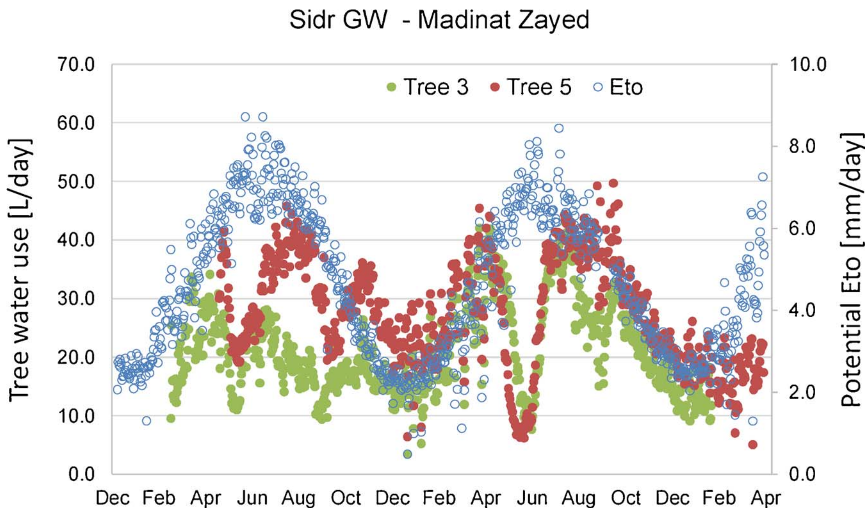

Fig. 9. The seasonal pattern of tree water use, T ($L\,d^{-1}$) by two Sidr trees (3 and 5) being irrigated with groundwater (GW), shown in relation to ETo ($mm\,d^{-1}$) over 2 years beginning in 2015.

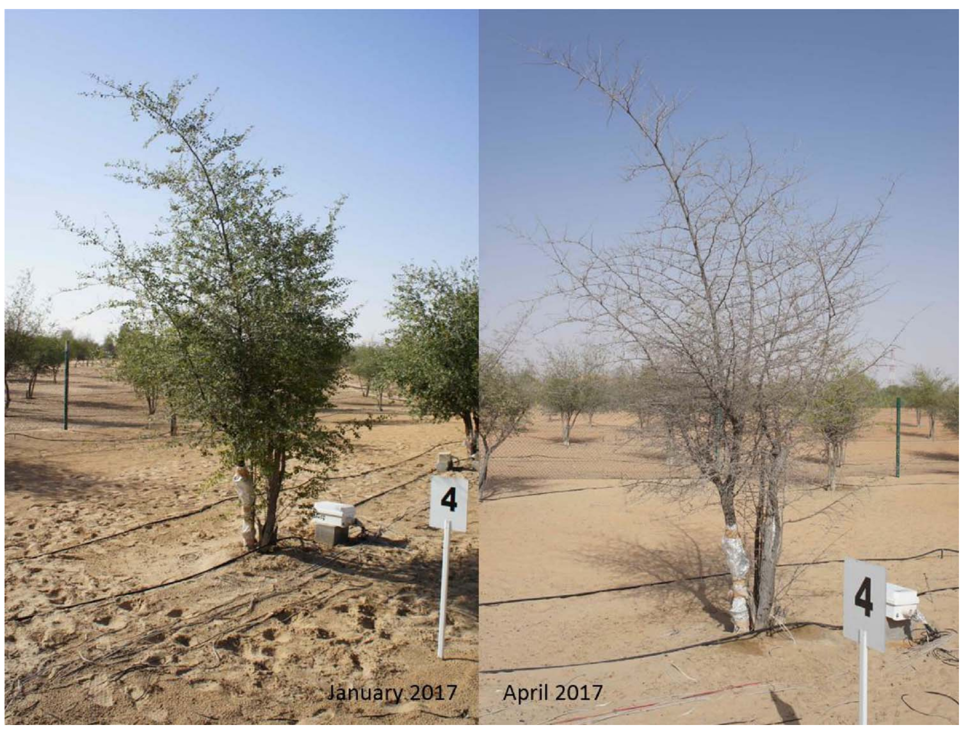

Fig. 10. The groundwater (GW) irrigated Sidr Tree 4 at full leaf in January 2017 (left). The same tree is shown in April on the right.

coefficient for the regressions are −0.29 and −1.22 respectively for Tree 3 and Tree 2, which suggests a simple arithmetic, annual-average for T, adjusted to the different tree sizes, would be better than using a unitary crop factor and a time-varying ETo!

It is instructive therefore to examine the seasonal pattern of daily tree water use, T, in relation to daily ETo, for all four monitored trees, and over the period of nearly 2.5 years of measurement. These data are shown in Fig. 5 here as the red dots, with ETo in blue.

The left-hand axes in Fig. 5 all have different scales, as the tree water use, T, of the two smallest trees (Trees 2 and 5) do not exceed 40 $L\,d^{-1}$, whereas the two larger trees use between 60 and 80 $L\,d^{-1}$. As alluded to in Fig. 4, the pattern of T diverges from ETo at distinct times of the year due to the deciduous behaviour of Al Ghaf. There is a period of leaf loss during June, which is most noticeable in Tree 3, and also in Trees 2 and 5. This is not quite so evident with Tree 4. Furthermore, the magnitude of this dip in T is different between years. For Tree 3 in 2015, the period of both leaf loss, and leaf regrowth in June was very sharp, covering about 25 days. Tree 4 in both years showed only weak deciduous behaviours. This complex and asynchronous behaviour leads to difficulties in applying a crop-factor approach to ETc prediction.

However, given the variation due to tree sizes, both within our experimental trees, and throughout the forest stand, an aggregated approach to defining Kc was adopted. The sap flow data from all four monitored trees was aggregated into average tree water-use values over the 2 years of experimentation, and these are shown in relation to ETo (Fig. 6). The linked patterns of T in $L\,d^{-1}$ and ETo in mm d^{-1} can be used to determine the temporal pattern of the crop factor. The impact of the varying asynchrony of leaf fall, flowering and new leaf growth, leads to a muted average pattern of T in relation to ETo.

The phenology of Al Ghaf trees is typically that new leaves appear just before, or simultaneously with, the fall of the old leaves. Flowering typically begins just after the flush of new leaves. This pattern of new

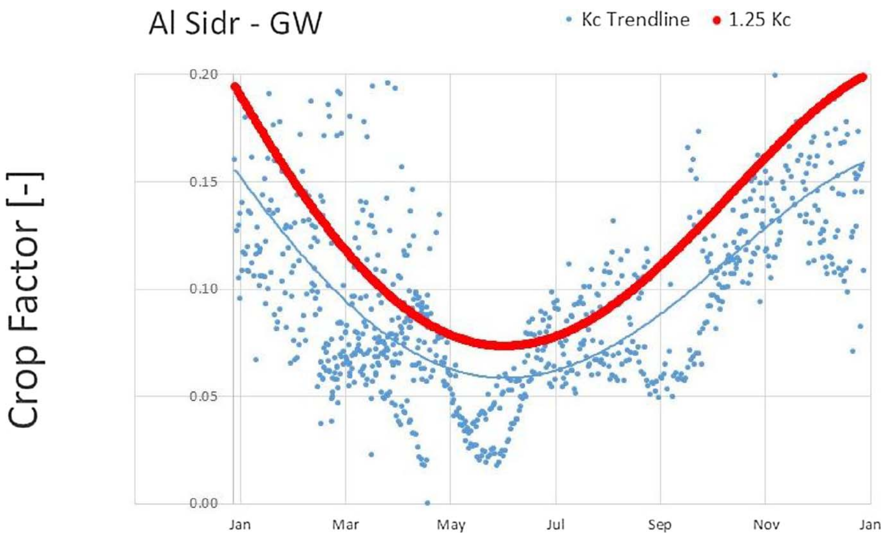

Fig. 11. The average daily crop-factor, *K*c, for the four instrumented Sidr trees over the year, computed from over 2 years of individual tree water-use *ET*c. The blue line is the fitted trendline using a 4th order polynomial. The red line is the fitted line with a 25% add-on as a 'factor-of-safety'. (For interpretation of the references to colour in this figure legend, the reader is referred to the web version of this article.)

Table 1
The seasonal pattern in maximum daily, *ET*o (mm d^{-1}), broken down by month at Madinat Zayed in the western desert of Abu Dhabi. For Al Ghaf trees (left) is shown the monthly maximum value of the crop factor, *K*c, along with the irrigation monthly requirements (L d^{-1}) considering a 25% factor-of-safety (1.25 *K*c. *ET*o) and a 25% salt-leaching factor (1.5 *K*c. *ET*o) for saline groundwater. On the right is shown these values for Al Sidr trees. The respective annual-average daily values are given at the foot of the table.

		Al Ghaf			Al Sidr		
Month	Average ETo (mm/day)	Maximum *K*c [–]	1.25 [*K*c .ETo] (L/day)	1.50 [*K*c .ETo] (L/day)	Maximum *K*c [–]	1.25 [*K*c .ETo] (L/day)	1.50 [*K*c .ETo] (L/day)
January	2.55	0.13	20.3	24.4	0.16	25.0	30.0
February	3.37	0.10	20.6	24.8	0.12	24.8	29.7
March	4.55	0.10	27.9	33.4	0.10	27.9	33.4
April	5.74	0.10	35.2	42.2	0.08	28.1	33.8
May	6.67	0.10	40.9	49.0	0.06	24.5	29.4
June	7.15	0.10	43.8	52.6	0.06	26.3	31.5
July	7.10	0.10	43.5	52.2	0.07	30.4	36.5
August	6.53	0.11	44.0	52.8	0.08	32.0	38.4
September	5.60	0.12	41.2	49.4	0.10	34.3	41.2
October	4.51	0.14	38.7	46.4	0.13	35.9	43.1
November	3.59	0.15	33.0	39.6	0.14	30.8	36.9
December	3.26	0.15	30.0	35.9	0.16	31.9	38.3
	Annual Average (L/day)		34.9	41.9		29.3	35.2

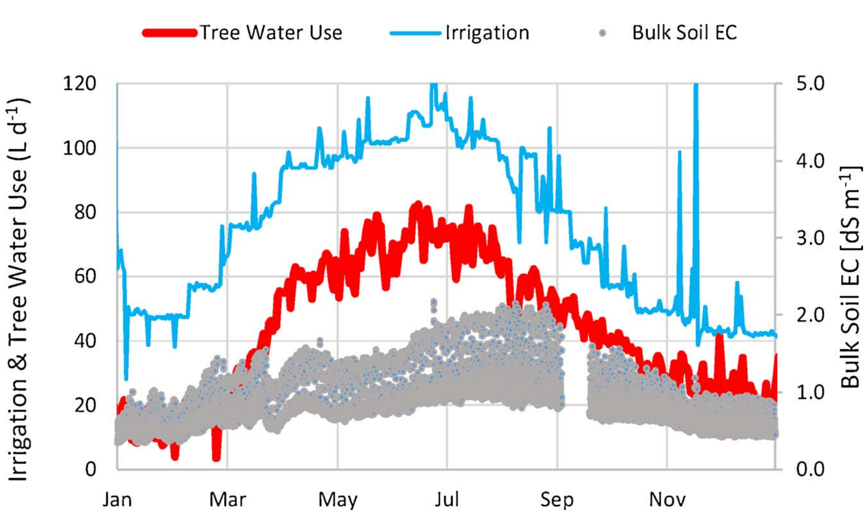

Fig. 12. The measured daily irrigation rate applied to Al Ghaf tree #4 from 25 January 2017 to 25 January 2018 (blue line), along with the tree water-use measured by sap-flow monitoring (*ET*c – red line). The monthly schedule was set to achieve an irrigation rate of 1.5 *ET*c to ensure a salt leaching fraction of 25%, with a factor-of-safety of 25%. The pattern in the bulk-soil electrical conductivity (EC), as measured by a CS 655 probe under the dripper, is also shown (grey dots). (For interpretation of the references to colour in this figure legend, the reader is referred to the web version of this article.)

foliage, flowering and fruiting occurs during the hottest period of the year between March and August. However, we have found that the relative strengths of the vegetative and flowering cycles varies in any given year between trees, and is due to the biennial bearing characteristic displayed by fruiting trees. In Fig. 7 we show photos of two neighbouring trees, Tree 3 (left) and Tree 4 (right), taken on the same day in 2017. Tree 3 can be seen to be having an 'on' year in relation to flowering, whereas as Tree 4 was having an 'off' for flowering. The relative vegetative vigour of the trees is different with Tree 4 showing a surge of new leaf growth. Elsewhere in our experimental plot of eight instrumented trees, four GW irrigated and four TSE irrigated, we observed five trees to be having 'on' years of flowering, and three with 'off' years of flowering. It is this asynchrony that leads to the muted seasonally deciduous pattern in the average *T* in relation to *ET*o (Fig. 6).

We can scale-up to the forest stand using the average pattern of *T*, relative to *ET*o, to compute the average crop factor *K*c. This is shown in Fig. 8. There is a weak seasonal deciduous pattern, on average. The crop factor drops in February–March as the trees begin to lose leaves as they initiate flowering. Then *K*c remains effectively constant until new leaf growth lifts the crop factor in September to its peak in December. This pattern in the average *K*c enables us to predict irrigation requirements for stands of Al Ghaf trees, as we show later.

3.2. Al Sidr transpiration

Our measured *ET*c for each of the four multi-stemmed Sidr trees is computed using our baseline measurements of sapflow in four measured stems. The flow in the measured stems was scaled to a flux density using the trunk cross-sectional area of the measured stems. The trees were then surveyed to find the diameters of all of the stems. The total trunk cross-sectional area of the whole tree was computed and the sap-flux density applied to this to compute the tree's total water use. The pattern of tree water use, *T*, is shown for Al Sidr Trees 3 and 5 in Fig. 9, along with the seasonal pattern over two years of *ET*o.

The impact of the deciduous behaviour of the Sidr trees is distinct and synchronous. There is a rapid loss of leaves in April, followed by rapid new leaf growth in May. There is a second, less distinct, period of leaf-loss in August with regrowth during September. Our measurements, and observations in the forest stand, reveal a greater degree of synchrony between trees, with less evidence of biennial bearing. In Fig. 10 we show how significant the deciduous behaviour in spring can be. On the left of Fig. 10 we show Sidr Tree 4 at the full-leaf stage in January 2017. By April, the tree has no leaves at all (Fig. 10, right). In the background of the April photo, it can be seen that most trees have either no leaves, or just a few.

The average crop factor *K*c was computed for all four trees, and the seasonal pattern over the year is shown in Fig. 11, using over two years of sapflow measurements. A strong seasonal pattern is found, albeit with a degree of variability due to some weak asynchrony and tree-to-tree variation. A 4th order polynomial was fitted to the data, and is shown in Fig. 11. The amplitude in the seasonal pattern of the average *K*c is large, ranging from 0.16 in December/January, down to 0.06 in summer. In contrast, the average *K*c for the Ghaf trees ranged from just 0.10–0.15.

3.3. Irrigation allocation and law 5

Current practice is to irrigate both the Ghaf and Sidr trees with $60\,L\,d^{-1}$ of groundwater. Implementation of Abu Dhabi's Law 5 requires that irrigation be allocated at the minimum amount required to achieve the desired goal. Our results here are being used to define the irrigation allocation under Law 5 for amenity plantings of Al Ghaf and Al Sidr trees. We use our fitted values of *K*c, broken down by the maximum value for every month, to determine firstly the water use of the trees with what we consider to be an equitable 25% factor-of-safety (Table 1). Because the trees are irrigated with GW at a salinity of 8–10 $dS\,m^{-1}$ we recommended that the irrigation allocation be at 1.5 *ET*c, so as to provide a 25% salt-leaching fraction.

We have assessed whether a salt-leaching fraction of 25%, with a factor-of-safety of 25%, is sufficient by monitoring the rootzone salinity of an Al Ghaf, and Al Sidr tree, during 2017, after imposing a monthly irrigation schedule of 1.5 *ET*c. We present the results for the Ghaf tree in Fig. 12. The irrigation schedule tracked 1.5 times the measured *ET*c, and the bulk electrical conductivity can be seen to rise from around 0.5–1 $dS\,m^{-1}$, prior to irrigation, up to about 1–2 $dS\,m^{-1}$. The pattern depends on the season due to the varying rootzone dynamics of wetting by irrigation, and extraction by the tree. However, there is no progressive rise in the bulk EC of the soil, as the bulk EC in January 2018 was the same as it was in January 2017. This indicates that an irrigation rate of 1.5 *ET*c is sufficient to flush excess salts from the rootzone.

The monthly pattern of irrigation requirements at 1.5 *ET*c shows that Al Ghaf trees will need, on average, just $24\,L\,d^{-1}$ during winter, and up to $53\,L\,d^{-1}$ in summer (Fig. 6). The annual-average daily water requirements will be $42\,L\,d^{-1}$, a saving of 30% on the current practice of $60\,L\,d^{-1}$. For the smaller Sidr trees, the water requirements are less, with the lowest water needs occurring in May at $30\,L\,d^{-1}$, and rising to $43\,L\,d^{-1}$ in October (Fig. 9). On annual average, the water requirement for Al Sidr is just $35\,L\,d^{-1}$, an annual saving of over 40% on current practice.

4. Conclusions

The arid forests in the hyper-arid deserts of Abu Dhabi require irrigating. Saline groundwater is the predominant source for the irrigation water, and current practice is to irrigate Al Ghaf and Al Sidr trees with design quantity of 60 L of groundwater every day of the year. Over-extraction of the Emirate's aquifers threatens groundwater sustainability. Consequently Law 5 has been passed in Abu Dhabi to restrict groundwater takes for irrigation to protect the subterranean reserves of water. Law 5 will prescribe allocation limits so that only the minimum amount of water is used to achieve the desired outcome. We have carried out experiments on Al Ghaf and Al Sidr trees in the western desert of Abu Dhabi using sap flow measurements to monitor tree water use over 2.5 years. These results were used to quantify the seasonal pattern in the crop factor, *K*c, for these two deciduous arid-forest species. The seasonal patterns between the two species are quite different, due to their idiosyncratic patterns of leaf fall, flowering and leaf regrowth. By using predicting tree water-use, *ET*c, as 1.5 *K*c.*ET*o, we could provide the regulations for Law 5 with irrigation allocation recommendations that included a 25% factor-of-safety, and a 25% salt-leaching fraction. These recommendations represent a 30% reduction on current practice for the groundwater irrigation of Al Ghaf trees, and a 40% saving for Al Sidr trees.

References

Al Mulla, M., 2011. UAE State of Water Report. Ministry of Environment and Water, Abu Dhabi.

Allen, 2018. Crop Evapotranspiration: Guidelines for Computing Crop Water Equirements. FAO Irrigation and Drainage Paper No 56. Food and Agriculture Organization of the United Nations, Rome.

Ankeny, M.D., Ahmed, M., Kaspar, T.C., Horton, R., 1991. Simple field method for determining unsaturated hydraulic conductivity. Soil Sci. Soc. Am. J. 55, 467–470.

Clothier, B.E., 1984. Solute travel times during trickle irrigation. Water Resour. Res. 20, 1848–1852.

Clothier, B.E., 2000. Infiltration. In: Smith, K.A., Mullins, C.E. (Eds.), Soil Analysis: Physical Methods. Marcel Dekker Ltd, pp. 235–276 (Chapter 6).

Dawoud, M., 2011. Water Resources and Their Economical Role in the United Arab Emirates (Arabic). Sultan Bin Zayed's Culture and Media Center, Abu Dhabi.

De Pauw, E., Gobel, W., Adam, H., 2000. Agrometeorological aspects of agriculture and forestry in the arid zones. Agric. For. Meteorol. 103 (1–2), 43–58. http://dx.doi.org/10.1016/s0168-1923(00)00118-0.

EAD, 2006. Trees and shrubs of forest areas of Abu Dhabi emirate.

EAD, 2009. Soil Survey of Abu Dhabi Emirate. vol I Extensive Survey, Environment Agency, Abu Dhabi.

EAD, 2016a. Abu Dhabi forests data [Statistical].

EAD, 2016b. Strategic Plan 2016–2020.

EAD, 2017. Water. EAD.

FAO, 2010. Global Forest Resources Assessment. Food and Agriculture Organization of the United Nations, Rome.

Green, S., Clothier, B., Jardine, B., 2003. Theory and practical application of heat pulse to measure sap flow. Agron. J. 95 (6), 1371–1379.

Green, S.R., Clothier, B.E., Perie, E., 2009. A re-analysis of heat pulse theory across a wide range of sap flows. Acta Hortic. 846, 95–104.

Hatton, T.J., Catchpole, E.A., Vertessy, R.A., 1990. Integration of sapflow velocity to estimate plant water-use. Tree Physiol. 6 (2), 201–209.

Khan, M.A., 1999. The Indigenous Trees of the United Arab Emirates. Dubai Municipality, Dubai.

Murad, A.A., Al Nuaimi, H., Al Hammadi, M., 2007. Comprehensive assessment of water resources. Water Resour. Manage. 21, 1449–1463.

Murad, A.A., 2010. An overview of conventional and non-conventional water resources in arid region: assessment and constrains of the United Arab Emirates (UAE). J. Water

Resour. Prot. 2 (2), 181–190.
Philip, J.R., 1984. Travel-times from buried and surface infiltration point sources. Water Resour. Res. 20 (7), 990–994. http://dx.doi.org/10.1029/WR020i007p00990.
Wooding, R.A., 1968. Steady infiltration from a shallow circular pond. Water Resourc. Res. 4 (6), 1259. http://dx.doi.org/10.1029/WR004i00 6p01259.